

Towards a test of quantum gravity with a levitated nanodiamond containing a spin

Benjamin D. Wood^a and Gavin W. Morley^a

^aDepartment of Physics, University of Warwick, Coventry, CV4 7AL, United Kingdom

ABSTRACT

There is significant interest in potential experimental tests of macroscopic quantum effects, both to test potential modifications to quantum theory and to probe the quantum nature of gravity. A proposed platform with which to generate the required macroscopic quantum spatial superposition is a nanodiamond containing a negatively charged nitrogen vacancy (NV^-) centre. In this review, methods to fabricate nanodiamonds containing NV^- suitable for these quantum applications are discussed. The proposed probes of the macroscopic limits of quantum theory are presented along with the spin physics of the NV^- centre relevant to those tests.

Keywords: Diamond, Nitrogen Vacancy Centre, Matter-Wave Interferometry, Quantum Foundations

1. INTRODUCTION

Levitated nanodiamond experiments have been proposed as a platform to probe the macroscopic limits of quantum theory¹⁻⁶ and the quantum nature of gravity.⁷⁻⁹ These experiments utilise the electronic spin of the negatively charged nitrogen vacancy (NV^-) defect in diamond. Whilst the levitated nanodiamond experiments suggested exhibit desirable features as a test of macroscopic superposition, there are still a number of challenges to be overcome before they are practically achievable. These include the short NV^- spin coherence (T_2) time in nanodiamonds compared to that of bulk diamond.

This review will provide a background to the synthesis of diamond, the optical and spin physics of the NV^- centre, and the specific methods of nanodiamond fabrication in Sec. 2, 3, and 4 respectively. Next, the proposed experimental tests of the macroscopic limits of quantum physics and proposed probes of the quantum nature of gravity are discussed in Sec. 5. Finally, the different methods of trapping nanodiamond in order to perform the levitated nanodiamond experiments are discussed in Sec. 6.

2. DIAMOND SYNTHESIS

Using synthetically grown diamond is advantageous for research purposes as the impurity content and crystal morphology can be controlled. This is in contrast to naturally formed diamond where, by its nature, the growth conditions cannot be controlled. There are two primary methods of bulk diamond synthesis, high pressure high temperature (HPHT) synthesis and chemical vapour deposition (CVD) synthesis. Both techniques allow the nitrogen content of the grown diamond to be controlled. This is important when trying to control the final NV^- defect concentration in a diamond sample.

Further author information:

B.D.W.: E-mail: ben.d.wood@warwick.ac.uk

G.W.M.: E-mail: gavin.morley@warwick.ac.uk

2.1 High Pressure High Temperature

One method to synthesise diamond is to place carbon in a high pressure high temperature (HPHT) environment with a metal solvent.¹⁰ The high temperatures and pressures are required as at room temperature and pressure the thermodynamically stable form of carbon is graphite, sp^2 bonded carbon. Here each carbon atom bonds to its three equidistant nearest neighbours in a plane. For higher pressures diamond, sp^3 bonded carbon, is the thermodynamically stable form. Each carbon bonds to four equidistant nearest neighbours in a tetrahedral structure.¹¹ Modern HPHT reactors typically operate in the parameter space of 1600–1900 K and 5–6 GPa,^{12–14} however synthesis at higher temperatures and pressures is possible.¹⁵

Nitrogen is the dominant impurity in HPHT diamond, forming mostly single substitutional nitrogen in typical HPHT reactors, however at extremely high temperatures the substitutional nitrogen can aggregate.¹⁶ The typical nitrogen concentrations incorporated into HPHT diamonds are approximately 200–300 ppm which can be further increased by adding nitrogen containing compounds to the growth mixture.

As well as adding compounds to increase the nitrogen incorporation into the final diamond material when trying to generate a high nitrogen content, it can be desirable to grow higher purity diamond where it is required to try and minimise the nitrogen content. This is achieved by adding a nitrogen ‘getter’ material into the carbon source material. This is typically Al or Ti metal as they both form stable nitrides.¹⁷

2.2 Chemical Vapour Deposition

An alternative diamond synthesis technique to HPHT is CVD. CVD is a technique to grow diamond material in the region of phase space where graphite is the thermodynamically stable form of carbon. Whilst this is not possible in the context of equilibrium thermodynamics, chemical kinetics allow sp^3 carbon to be preferentially grown over sp^2 carbon.¹⁸

The CVD process utilises mostly H and C containing source gases along with a growth seed. The source gases are dissociated into their radical components by transferring energy to the gas mixture. This can be done either by a hot filament running close to the growth seed,¹⁹ or by placing the seed within a microwave resonator cavity.²⁰ The microwave radiation or hot filament ignites a plasma of gas radicals at low pressure, < 1 atm.¹² The typical CVD growth process involves hydrogen radicals etching carbon-hydrogen bonds on the surface of the diamond growth, then the majority of the time a hydrogen radical will reform the C-H bond. However, sometimes a carbon radical can be captured by the dangling bond, forming a C-C bond. This bonding can initially be sp^2 or sp^3 , but sp^2 bonds are etched away by H radicals faster than the etch rate of sp^3 bonded carbon.^{12,20} This generates a net rate of growth of diamond material.

By adding N containing gases to the H and C containing source gases, with precise control, CVD-grown single crystal diamonds with single substitutional nitrogen content ranging from < 0.5 ppb to > 1 ppm are available commercially. The high purity achievable by the CVD technique has made CVD-produced diamonds a useful platform for quantum applications, in particular quantum sensing.²¹

3. NITROGEN VACANCY CENTRE

The nitrogen vacancy (NV) centre is a defect in the carbon lattice of diamond. It consists of a substitutional nitrogen atom on a lattice site in diamond that has a vacant lattice site as one of its nearest neighbours.²² The electronic structure of the neutral defect (NV^0) is made up of three electrons contributed from dangling carbon bonds around the vacancy, and two contributed from the valence electrons in nitrogen after forming three bonds with adjacent carbons.²³ NV^0 can accept an electron from a donor species in the carbon lattice to form the negatively charged NV^- variant of the nitrogen vacancy centre.¹² The NV^- centre is the subject of growing interest in the fields of magnetometry,²² quantum networking and computing,²⁴ and probes of fundamental physics.^{1–3,5}

The NV^- centre can be found as a grown-in defect from the chemical vapour deposition (CVD) diamond growth process or it can be created in existing diamond material.²⁵ The details of these methods of NV creation are covered in Sec. 4.1.

The NV^- centre is an electronic spin-1 system,²⁵ with energy levels shown in Fig. 1. The ground state spin triplet, 3A_2 , has a zero field splitting of 2.87 GHz.²⁵

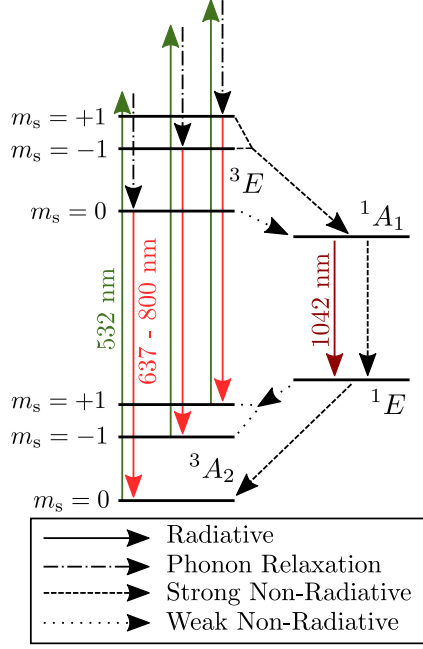


Figure 1. Energy level diagram of the NV⁻ centre. The degenerate $m_s = \pm 1$ levels are zero-field split from $m_s = 0$. Degeneracy is broken by application of an external magnetic field. Under 532 nm excitation the relative strengths of non-radiative transitions mean that initially the strength of 637 – 800 nm fluorescence can be used to readout the spin state, and that after continued excitation the spin state is polarised to $m_s = 0$.

3.1 Optically Induced Spin Polarisation

The NV⁻ centre exhibits optically induced spin polarisation; the process is depicted in Fig. 1. To optically polarise, first excite the NV⁻ with 532 nm laser light. This drives the system from the ground 3A_2 state to the phonon band of the 3E excited state. This optical transition is spin preserving.²² After the excitation, the electron will quickly undergo phonon relaxation and fall to the corresponding zero-phonon $m_s = \pm 1$ or 0 spin state of the 3E level.

In the case that the ground state electron was initially in the state $m_s = 0$, the most likely channel of decay to the ground state is through a spin-preserving optical transition back to the $m_s = 0$ spin state of the 3A_2 level.^{25,26} This transition emits a photon into the 637 nm zero phonon line (ZPL) of the NV⁻ centre, or into the phonon sideband of the 637 nm ZPL that extends to ≈ 800 nm.²⁷ In this case the system remains in the $m_s = 0$ spin state and will undergo cycles of photoluminescence when excited by 532 nm light.

In the case that the system was originally in the $m_s = +1$ or -1 state, the non-radiative inter-system crossing (ISC) decay channel from the $m_s = \pm 1$ excited states to the 1A_1 energy level is significantly more likely than the system undergoing ISC from the $m_s = 0$ excited state.^{25,26} From the 1A_1 energy level, the system undergoes a transition to the 1E state. Finally the system undergoes another ISC transition to the $m_s = 0$ or $m_s = \pm 1$ 3A_2 ground state with approximately equal probability.^{25,26} Therefore under continued 532 nm excitation the NV⁻ centre spin polarises to the $m_s = 0$ state.

Other decay channels are possible, as shown in Fig. 1, therefore the exact degree of polarisation that can be achieved is variable, with values from 42% – 96% reported.²⁵

3.2 Microwave Control

To manipulate the spin state of the NV⁻ centre, a static magnetic field is applied to the host diamond. This splits the otherwise degenerate $m_s = \pm 1$ levels due to Zeeman splitting.²² The $m_s = \pm 1$ states move away from the zero magnetic field state at ± 28.02 MHz mT⁻¹.²⁸ An applied microwave field, tuned to be resonant either with the $m_s = 0 \leftrightarrow +1$ or $m_s = 0 \leftrightarrow -1$ transition, will flip the spin state.

3.3 Spin Dependant Fluorescence

To readout the spin state of the NV^- centre, optical detection is typically used. If the NV^- centre spin state is in $m_s = 0$, as a 532 nm excitation is switched on the NV^- centre will produce photoluminescence in the 637 nm – 800 nm range. This is due to the $m_s = 0$ state cycling from excited state to ground state as described in Sec. 3.1. If the NV^- centre is in the $m_s = +1$ or -1 state and the 532 nm excitation is switched on, before the spin state optically polarises the 637 nm – 800 nm photoluminescence produced will be of a lower intensity than for the $m_s = 0$ case. Also the ${}^3\text{E}$, $m_s = 0$ optical decay lifetime is 23 ns in nanodiamond²⁹ and 12 ns in bulk,²⁵ whereas the limiting decay lifetime of the ${}^1\text{A}_1$, ${}^1\text{E}$ pair of levels is ≈ 300 ns.²² Therefore, the $m_s = \pm 1$ state gets ‘stuck’ in the long lifetime ${}^1\text{A}_1$, ${}^1\text{E}$ decay channel, further decreasing the photoluminescence signal.

By exciting the NV^- centre with 532 nm laser light, frequency sweeping a microwave signal to manipulate the NV^- spin state and detecting 637 nm – 800 nm emission the techniques of optically-induced spin polarisation, microwave control, and spin dependant fluorescence are used to facilitate optically detected magnetic resonance (ODMR). An example ODMR spectrum of the NV^- centre is shown in Fig. 2 of Ref. 22.

3.4 Power Saturation

The photoluminescent emission of NV^- centres exhibits saturation as the excitation intensity increases, see Fig. 5 of Ref. 30. There is a maximum number of excitation and decay cycles that can occur per second, due to the finite state lifetimes, limiting the maximum emission count rate no matter how much power the excitation laser delivers. The emitted photon count rate I as a function of excitation power P is fit with eqn. 1:³¹

$$I = I_\infty \frac{P}{P_{\text{Sat}} + P} \quad (1)$$

where I_∞ and P_{Sat} are the photon count rate for infinite excitation power and the excitation saturation power respectively.

3.5 Photon Correlation

To determine whether observed signals originate from a single NV^- centre a Hanbury Brown-Twiss (HBT) measurement is used^{32,33}. The emitted photons are split into two channels, each of which are detected as clicks in single photon detectors, and the time of detection logged. By histogramming the time delay between a click in one channel and a click in the other the degree of correlation between photons with a given delay time can be established. The second order correlation function, $g^{(2)}(\tau)$, for this process is given by eqn. 2:³⁴

$$g^{(2)}(\tau) = \frac{\langle I(t+\tau)I(t) \rangle}{\langle I(t) \rangle^2} \quad (2)$$

where τ is the time delay between two clicks, and $I(t)$ is the electromagnetic energy absorbed by a detector at time t . $\langle \dots \rangle$ indicates that the process is averaged over time. $g^{(2)}(\tau) > 1$ indicates a positive correlation between photon detection events separated by τ , $g^{(2)}(\tau) < 1$ indicates negative correlation, see Fig. 6 of Ref. 30, and $g^{(2)}(0) = 0$ indicates that two photons were never detected simultaneously, one at each detector.³⁴ A single NV^- centre can only emit one photon at a time, so ideally $g^{(2)}(0) = 0$. An ideal pair of NV^- centres exhibit $g^{(2)}(0) = 0.5$, therefore allowing for noise a single centre is identified if $g^{(2)}(0) < 0.5$.³³

3.6 Spin Coherence Time

The electron spin coherence time, T_2 , of the NV^- centre is a measure of the time that the spin can store a quantum state without it decohering due to other NV spins in its local environment.³⁵ The T_2 time can be measured directly by initialising the NV^- into the $m_s = 0$ state, applying a Hahn echo microwave pulse sequence,³⁶ and using spin-dependant fluorescence to readout the degree of coherence of the NV^- spin state.

The T_2 time places a limit on the macroscopicity of spatial superposition that can be created using the proposed methods of Sec. 5.1. The T_2 time can be extended by, instead of using a simple Hahn echo pulse sequence, using a dynamical decoupling pulse sequence that better decouples the NV^- spin from the local spin environment. For example the CPMG or XY8 dynamical decoupling sequences^{33,37,38} act to cancel the phase

contributions of environmental spins. To maximise the T_2 time, pulse sequences containing on the order of $10^3 - 10^4 \pi$ pulses are required.³⁷ Figure 11 of Ref. 33 shows an number of example measurements of the T_2 time of a single NV^- electronic spin using the Hahn echo pulse sequence.

One source of decoherence is from the spin- $\frac{1}{2}$ ^{13}C nuclei³⁹ that occur naturally in diamond with 1.1% abundance.⁴⁰ Other factors can also contribute to limiting T_2 time, such as the concentration of substitutional nitrogen defects and the degree to which the external static magnetic field used to induce Zeeman splitting, see Sec. 3.2, is aligned with the NV^- axis.⁴¹ If the field is off axis the $m_s = 0, \pm 1$ states are no longer the eigenstates of the NV^- spin, causing additional decoherence.

The longest NV^- electron spin T_2 time measured is 1.58 s using a < 5 ppb nitrogen concentration, CVD grown, bulk diamond cooled to 3.7 K.⁴² The observed T_2 times in nanodiamonds are significantly shorter than those for bulk diamond. A proposed explanation for these differences is that impurities and dangling bonds at the diamond surface can modify the charge transport properties at the surface, causing an increase in the number of NV^- centres that are charge switched to their neutrally charged counterpart.⁴³ Charge transport can also induce electric field noise at the NV^- centre, along with surface spin flips that induce magnetic field noise. Both of these noise sources reduce the nanodiamond T_2 time.

The longest T_2 time in nanodiamonds, using CVD growth and lithography techniques to manufacture isotopically pure ^{12}C diamond cylinders of diameter ≈ 500 nm and length $\approx 1 \mu m$, is $T_2 = 708 \mu s$ when using dynamical decoupling techniques.⁴⁴ For natural abundance ^{13}C nanodiamonds, the longest T_2 time reported is $462 \mu s$ measured in nanodiamonds produced by CVD growth and milling.⁵ The nanodiamond containing the NV^- with $T_2 = 462 \mu s$ had diameter ≈ 200 nm. Both of these measurements were made at room temperature.

4. NANODIAMOND CONTAINING NV^-

4.1 NV^- Creation

The NV centre can be found as a grown-in defect from the chemical vapour deposition (CVD) diamond growth process,⁴⁵ or created as a product of particle irradiation and annealing,⁴⁶ as a product of nitrogen ion implantation and annealing,⁴⁷ and by laser writing.⁴⁸

In both the irradiation and ion implantation cases the principle of the process is the same. The methods ensure that substitutional nitrogen and vacancy sites are present in the diamond lattice, then an anneal at $> 600^\circ C$ makes the vacancies mobile in the diamond lattice.^{46,49} The vacancies can move until they are trapped by a substitutional nitrogen, forming an NV centre. The centres form in the NV^- or NV^0 charge states⁴⁶ and therefore trying to maximise the creation of NV^- over NV^0 is important when the diamond is to be used for NV^- applications. Despite vacancies being mobile for temperatures $> 600^\circ C$ it has been observed that the annealing temperatures to maximise the number of NV centres produced are those $> 800^\circ C$.^{50,51}

In the irradiation case, vacancies are formed by high energy particle irradiation and the substitutional nitrogen content is provided by the grown-in nitrogen content of the diamond sample. The density of NV centre creation is limited by the concentration of grown-in substitutional nitrogen. In the ion implantation case, nitrogen ions are implanted into the diamond lattice.⁵² This process has the benefit of allowing the final substitutional nitrogen content to be controlled, and the kinetics of implanting nitrogen ions will also create vacancy centres in the same region.

Laser writing of NV centres differs slightly from the processes discussed above. Vacancy centres are created in the lattice by using a focused, high energy, laser pulse. A global anneal in a furnace^{33,48} or a pulse train of lower energy pulses follows the initial vacancy-creating pulse to anneal the area local to the created vacancy.⁵³ Laser-written NV^- centres can have T_2 times³³ and optical coherence⁴⁸ as good as naturally occurring NV^- .

4.2 Nanodiamond Fabrication

There are two primary methods of nanodiamond fabrication for quantum applications. The first method of nanodiamond production is to synthesise a macroscopic parent diamond sample, either by HPHT⁵⁴ or CVD⁵⁵ methods, and then to mechanically mill the sample into nano-scale particles.⁵⁶ In this scheme the NV^- concentration in the parent diamond sample and the final size of the nanodiamond particles sets the probability that

a nanodiamond contains a certain number of NV^- centres. Typically when creating nanodiamonds with the aim of measuring a long $NV^- T_2$ time, the parameters are chosen such that the probability of a nanodiamond containing any NV^- centres is low. This is because having pure diamond material is desired and measurements can be repeated until a nanodiamond containing an NV^- is found experimentally.

The other method for nanodiamond fabrication is based on etching of a specifically grown parent sample. It can be used to create nanodiamonds with tailored shape and size.⁴⁴ One example is the use of electron beam lithography to pattern an etch mask onto a sample of CVD grown diamond membrane that includes a ~ 6 nm thick NV^- defect layer in the centre of the vertical profile of the membrane. The prepared sample is then plasma etched. This removes the material in the unmasked regions. The mask pattern used results in cylindrical nanodiamond particles that are $\sim 1 \mu\text{m}$ in depth and ~ 500 nm in diameter.

Comparing the two methods, a disadvantage of the milling technique over etching techniques is that there is no control over the placement of the NV^- within the nanodiamond or the final shape of the nanodiamond particle, however unlike etching, milling techniques allow creation of nanodiamonds from the full 3D volume of the bulk material at once. It is therefore easier to create large quantities of nanodiamonds with milling. In trapping applications where nanodiamonds are loaded by spraying,⁵⁷ the large number of nanodiamonds created in one milling run is beneficial as thousands of nanodiamonds are sprayed to trap one.

5. QUANTUM LIMITS

Quantum mechanics is a hugely successful theory, however there are still elements that warrant further experimental investigation. For instance, quantum theory places no limit on the allowed macroscopicity of superpositions, however molecules containing around 2000 atoms have demonstrated the most macroscopic superposition as yet observed.⁵⁸⁻⁶⁰

The lack of observation of macroscopic superposition could be explained by larger systems not being isolated from the environment well enough, however, there are also a number of proposed modifications to quantum mechanics. A family of modifications can be described as spontaneous collapse models, for example continuous spontaneous localisation (CSL), where terms added to the evolution can spontaneously collapse superposition states with a characteristic rate and length scale.^{61,62} By observing more macroscopic superpositions in the lab, bounds can be placed on the parameters of the proposed modifications to quantum theory.

The degree to which an experimental observation bounds the time scale of spontaneous collapse, given the length scale of the experiment, can be used to define a measure of the macroscopicity of the superposition.⁶³ It is by this measure that the 2000 atom experiment referenced previously is the most macroscopic.⁶⁰

Another outstanding issue with quantum theory is the difficulty of combining it with general relativity. To date, there is a lack of experimental observations that probe the quantum nature of gravity that can be used to help guide theoretical investigation. One such probe of the quantum nature of gravity would be an experiment that could determine whether the gravitational interaction can entangle two quantum states.^{8,9}

5.1 Experimental Tests

The use of levitated nanodiamond particles to probe the limits of the quantum superposition principle has been proposed.¹⁻⁶ The nanodiamond particle containing an NV^- centre is levitated and then the NV^- spin is manipulated to create a $m_s = \pm 1$ spin superposition state.

A magnetic field gradient is applied to the nanodiamond containing the NV^- centre. The gradient exerts a force on the NV^- spin magnetic moment in opposite directions depending on the $m_s = \pm 1$ state. This places the nanodiamond into a spatial superposition, as shown in Fig. 2(a), and allows the nanodiamond to be used as a matter-wave interferometer. This Stern-Gerlach interferometry has been demonstrated experimentally for a Bose-Einstein condensate.^{65,66}

By applying the magnetic field gradient at a variable angle with respect to the horizontal^{1,2,5} the nanodiamond superposition could be directly detected, due to the accumulated phase difference as the two nanodiamond positions in the superposition experience different gravitational potential energies. The phase difference would

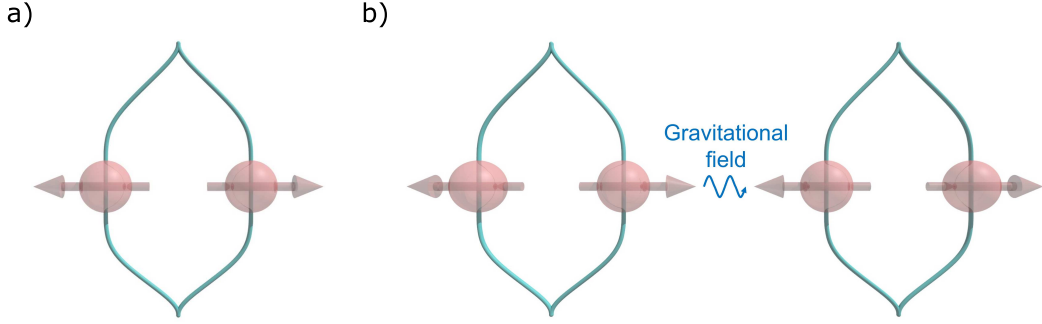


Figure 2. Schematics of the proposed schemes to test the limits of quantum mechanics with nanodiamonds containing NV^- . (a) To test the macroscopic limits of superposition, a magnetic field gradient would act on an NV^- spin superposition creating a superposition of forces, spatially splitting the superposition components into a spatial superposition of the nanodiamond.¹⁻⁶ The spatial superposition would then be recombined such that at the end of the scheme the spin state could be readout optically. After multiple runs with different tilts of the experiment with respect to the vertical defined by gravity, a spin interference fringe pattern would evidence the presence of the spatial superposition.^{1,2,5} (b) To probe the quantum nature of gravity, a pair of macroscopic spatial superpositions would be created simultaneously in close proximity to each other. If the distances involved are of the required magnitudes, the gravitational interaction between the two superposition components at the closest approach of the two nanodiamonds is dominant over the gravitational interaction between other pairs of superposition components.^{8,9} In this case the two NV^- spin states could be entangled if the gravitational interaction is quantum in nature.^{8,9,64}

be measured as an interference pattern of the final NV^- spin state once the two superposition components have been re-combined.

The proposals include schemes in which the nanodiamond is trapped, or in free fall. The trapped schemes are closer to being practically achieved, and could be used to observe matter-wave interference of a large mass ($\approx 1 \times 10^{-17}$ kg) nanodiamond,¹ however, the superposition distance is limited, limiting the macroscopicity. The free fall schemes can increase the achievable superposition distance such that the macroscopicity of those experiments would be among the largest proposed to date and bounds could be tightened on the parameters of the CSL modification to quantum mechanics.^{2,4,5}

Alongside tests of macroscopic superposition it has also been proposed that nanodiamonds containing NV^- centres could be used to verify the quantum nature of gravity by checking for gravitational entanglement effects.^{8,9,64} This type of experiment will require a pair of nanodiamonds to both be placed into highly macroscopic superpositions within gravitational interaction range of each other, as shown in Fig. 2(b). Beyond the experimental challenges of generating a single superposition with a large separation for a long time,^{5,67} it is crucial to ensure entanglement could only have been generated by gravitational effects rather than other interactions, such as casimir forces.⁶⁸⁻⁷¹

6. NANODIAMOND LEVITATION

6.1 Optical Traps

Optical traps can levitate nanodiamonds by inducing an electric dipole in the trapped particle. The electric dipole is then confined at the focal point of a high intensity laser beam, with trapping powers typically of the order of 100 mW.^{55,72-75} It was observed that the total photoluminescence rate measured from the NV^- centre, and the ODMR contrast, decreased as the trapping laser power increased.⁷⁴ The high intensity laser could cause ionisation of the NV^- centre to NV^0 , reducing the measured NV^- photoluminescence.⁷⁴ The internal temperature of the nanodiamond can increase due to the heating effect of the trapping laser. Minimising heating as a source of decoherence in proposed tests of quantum superposition is crucial and so optical traps are no longer the ubiquitously suggested trapping mechanism in experimental proposals using levitated nanodiamonds.

6.2 Paul Traps

Paul traps create a radio frequency oscillating electric field to confine a charged particle. There are a number of different electrode designs that satisfy this requirement, with those that have been used to trap nanodiamonds including a needle electrode design,⁷⁶ an end cap geometry,⁷⁷ linear trap,⁷⁸ and a ring design.^{79–81} Like magnetic and magneto-gravitational traps, a key advantage of Paul traps over optical trapping is that the radio frequency electric fields generated by the trap are scattering free, that is the trapped particles are not heated by the trap itself.⁷⁶ In all cases the nanodiamonds have to be charged before loading into the Paul trap to allow trapping.

6.3 Magnetic Field Based

Magnetic traps utilise the diamagnetic nature of diamond to passively, stably trap a nanodiamond in three dimensions using a carefully-shaped magnetic potential. In this case, paramagnetic materials still cannot be stably trapped, however, diamagnetic materials can be stably trapped.⁸² A trap design that contains a nanodiamond particle using only magnetic fields has been demonstrated. Two rare earth magnets are machined to sharp points and brought to a vertical separation of $\approx 30\ \mu\text{m}$ from each other, achieving trapping frequencies of $\approx 400\ \text{Hz}$ vertically and $\approx 200\ \text{Hz}$ horizontally.⁸³

Magneto-gravitational traps, like magnetic traps, trap the nanodiamond using static magnetic fields, however, only in two dimensions. Trapping in the third dimension is achieved in combination with the gravitational potential. Magneto-gravitational trapping has been demonstrated for nanodiamond with trap frequencies of $\approx 100\ \text{Hz}$ in the magnetically confined directions and $\approx 10\ \text{Hz}$ in the gravitationally confined direction (long axis).⁵⁷

7. CONCLUSION

In conclusion, we have reviewed the literature concerning proposed experimental tests of the macroscopic limits of quantum theory, and the quantum nature of gravity, that suggest the use of a nanodiamond containing an NV^- centre as a platform to generate the required macroscopic spatial superposition. Along with discussions of the proposed experiments, methods of diamond synthesis, nanodiamond fabrication, and the spin physics of the NV^- centre relevant to the proposed experiments have been presented.

ACKNOWLEDGMENTS

The authors would like to thank James March and Myungshik Kim for discussions that improved the manuscript. G. W. M. is supported by the Royal Society.

REFERENCES

- [1] Scala, M., Kim, M. S., Morley, G. W., Barker, P. F., and Bose, S., “Matter-Wave Interferometry of a Levitated Thermal Nano-Oscillator Induced and Probed by a Spin,” *Phys. Rev. Lett.* **111**(18), 180403 (2013).
- [2] Wan, C., Scala, M., Morley, G. W., Rahman, A. A., Ulbricht, H., Bateman, J., Barker, P. F., Bose, S., and Kim, M. S., “Free Nano-Object Ramsey Interferometry for Large Quantum Superpositions,” *Phys. Rev. Lett.* **117**(14), 143003 (2016).
- [3] Wan, C., Scala, M., Bose, S., Frangeskou, A. C., Rahman, A. A., Morley, G. W., Barker, P. F., and Kim, M. S., “Tolerance in the Ramsey interference of a trapped nanodiamond,” *Phys. Rev. A* **93**(4), 043852 (2016).
- [4] Pedernales, J. S., Morley, G. W., and Plenio, M. B., “Motional dynamical decoupling for interferometry with macroscopic particles,” *Phys. Rev. Lett.* **125**, 023602 (2020).
- [5] Wood, B. D., Stimpson, G. A., March, J. E., Lekhai, Y. N. D., Stephen, C. J., Green, B. L., Frangeskou, A. C., Ginés, L., Mandal, S., Williams, O. A., Bose, S., and Morley, G. W., “Matter and spin superposition in vacuum experiment (MASSIVE),” arXiv:2105.02105 (2021).
- [6] Yin, Z.-q., Li, T., Zhang, X., and Duan, L. M., “Large quantum superpositions of a levitated nanodiamond through spin-optomechanical coupling,” *Phys. Rev. A* **88**(3), 033614 (2013).

- [7] Albrecht, A., Retzker, A., and Plenio, M. B., “Testing quantum gravity by nanodiamond interferometry with nitrogen-vacancy centers,” *Phys. Rev. A* **90**(3), 033834 (2014).
- [8] Bose, S., Mazumdar, A., Morley, G. W., Ulbricht, H., Toroš, M., Paternostro, M., Geraci, A. A., Barker, P. F., Kim, M. S., and Milburn, G., “Spin Entanglement Witness for Quantum Gravity,” *Phys. Rev. Lett.* **119**(24), 240401 (2017).
- [9] Marletto, C. and Vedral, V., “Gravitationally Induced Entanglement between Two Massive Particles is Sufficient Evidence of Quantum Effects in Gravity,” *Phys. Rev. Lett.* **119**(24), 240402 (2017).
- [10] Bundy, F. P., Hall, H. T., Strong, H. M., and Wentorf, R. H., “Man-Made Diamonds,” *Nature* **176**(4471), 51–55 (1955).
- [11] Bundy, F. P., Bassett, W. A., Weathers, M. S., Hemley, R. J., Mao, H. U., and Goncharov, A. F., “The pressure-temperature phase and transformation diagram for carbon; updated through 1994,” *Carbon* **34**(2), 141 – 153 (1996).
- [12] Ashfold, M. N. R., Goss, J. P., Green, B. L., May, P. W., Newton, M. E., and Peaker, C. V., “Nitrogen in diamond,” *Chem. Rev.* **120**(12), 5745–5794 (2020).
- [13] Strömman, C. V. H., Tshisikhawe, F., Hansen, J. O., and Burns, R. C., “Synthesis of diamond,” (2006). Patent: WO/2006/061672.
- [14] Schmetzer, K., “High pressure high temperature treatment of diamonds — a review of the patent literature from five decades (1960–2009),” *J. Gemm.* **32**, 52–65 (2010).
- [15] Palyanov, Y. N., Borzdov, Y. M., Kupriyanov, I. N., Bataleva, Y. V., Khokhryakov, A. F., and Sokol, A. G., “Diamond crystallization from an antimony–carbon system under high pressure and temperature,” *Cryst. Growth Des.* **15**(5), 2539–2544 (2015).
- [16] Chrenko, R. M., Tuft, R. E., and Strong, H. M., “Transformation of the state of nitrogen in diamond,” *Nature* **270**(5633), 141–144 (1977).
- [17] Strong, H. M. and Chrenko, R. M., “Diamond growth rates and physical properties of laboratory-made diamond,” *J. Phys. Chem.* **75**(12), 1838–1843 (1971).
- [18] Angus, J. C., Will, H. A., and Stanko, W. S., “Growth of Diamond Seed Crystals by Vapor Deposition,” *J. Appl. Phys.* **39**(6), 2915–2922 (1968).
- [19] Haubner, R. and Lux, B., “Diamond growth by hot-filament chemical vapor deposition: state of the art,” *Diam. Relat. Mater.* **2**(9), 1277–1294 (1993).
- [20] Tallaire, A., Achard, J., Silva, F., Brinza, O., and Gicquel, A., “Growth of large size diamond single crystals by plasma assisted chemical vapour deposition: Recent achievements and remaining challenges,” *C. R. Physique* **14**(2-3), 169–184 (2013).
- [21] Achard, J., Jacques, V., and Tallaire, A., “Chemical vapour deposition diamond single crystals with nitrogen-vacancy centres: a review of material synthesis and technology for quantum sensing applications,” *J. Phys. D: Appl. Phys.* **53**(31), 313001 (2020).
- [22] Rondin, L., Tetienne, J.-P., Hingant, T., Roch, J.-F., Maletinsky, P., and Jacques, V., “Magnetometry with nitrogen-vacancy defects in diamond,” *Rep. Prog. Phys.* **77**(5), 056503 (2014).
- [23] Larsson, J. A. and Delaney, P., “Electronic structure of the nitrogen-vacancy center in diamond from first-principles theory,” *Phys. Rev. B* **77**(16), 165201 (2008).
- [24] Awschalom, D. D., Hanson, R., Wrachtrup, J., and Zhou, B. B., “Quantum technologies with optically interfaced solid-state spins,” *Nat. Photonics* **12**(9), 516–527 (2018).
- [25] Doherty, M. W., Manson, N. B., Delaney, P., Jelezko, F., Wrachtrup, J., and Hollenberg, L. C. L., “The nitrogen-vacancy colour centre in diamond,” *Phys. Rep.* **528**(1), 1–45 (2013).
- [26] Robledo, L., Bernien, H., van der Sar, T., and Hanson, R., “Spin dynamics in the optical cycle of single nitrogen-vacancy centres in diamond,” *New J. Phys.* **13**(2), 025013 (2011).
- [27] Beha, K., Fedder, H., Wolfer, M., Becker, M. C., Siyushev, P., Jamali, M., Batalov, A., Hinz, C., Hees, J., Kirste, L., Obloh, H., Gheeraert, E., Naydenov, B., Jakobi, I., Dolde, F., Pezzagna, S., Twitchen, D., Markham, M., Dregely, D., Giessen, H., Meijer, J., Jelezko, F., Nebel, C. E., Bratschitsch, R., Leitenstorfer, A., and Wrachtrup, J., “Diamond nanophotonics,” *Beilstein J. Nanotechnol.* **3**, 895–908 (2012).

- [28] Sangtawesin, S., McLellan, C. A., Myers, B. A., Bleszynski Jayich, A. C., Awschalom, D. D., and Petta, J. R., “Hyperfine-enhanced gyromagnetic ratio of a nuclear spin in diamond,” *New J. Phys.* **18**(8), 083016 (2016).
- [29] Neumann, P., Kolesov, R., Jacques, V., Beck, J., Tisler, J., Batalov, A., Rogers, L., Manson, N. B., Balasubramanian, G., Jelezko, F., and Wrachtrup, J., “Excited-state spectroscopy of single NV defects in diamond using optically detected magnetic resonance,” *New J. Phys.* **11**(1), 013017 (2009).
- [30] Jelezko, F. and Wrachtrup, J., “Single defect centres in diamond: A review,” *Phys. Status Solidi A* **203**(13), 3207–3225 (2006).
- [31] Plakhotnik, T. and Aman, H., “NV-centers in nanodiamonds: How good they are,” *Diam. Relat. Mater.* **82**, 87–95 (2018).
- [32] Hanbury Brown, R. and Twiss, R. Q., “A Test of a New Type of Stellar Interferometer on Sirius,” *Nature* **178**(4541), 1046–1048 (1956).
- [33] Stephen, C. J., Green, B. L., Lekhai, Y. N. D., Weng, L., Hill, P., Johnson, S., Frangeskou, A. C., Diggle, P. L., Chen, Y.-C., Strain, M. J., Gu, E., Newton, M. E., Smith, J. M., Salter, P. S., and Morley, G. W., “Deep Three-Dimensional Solid-State Qubit Arrays with Long-Lived Spin Coherence,” *Phys. Rev. Appl.* **12**(6), 064005 (2019).
- [34] Berthel, M., Mollet, O., Dantelle, G., Gacoin, T., Huant, S., and Drezet, A., “Photophysics of single nitrogen-vacancy centers in diamond nanocrystals,” *Phys. Rev. B* **91**(3), 035308 (2015).
- [35] Wang, X. R., Zheng, Y. S., and Yin, S., “Spin relaxation and decoherence of two-level systems,” *Phys. Rev. B* **72**(12), 121303 (2005).
- [36] Hahn, E. L., “Spin Echoes,” *Phys. Rev.* **80**(4), 580–594 (1950).
- [37] Bar-Gill, N., Pham, L. M., Jarmola, A., Budker, D., and Walsworth, R. L., “Solid-state electronic spin coherence time approaching one second,” *Nat. Commun.* **4**, 1743 (2013).
- [38] Wang, Z.-H., de Lange, G., Ristè, D., Hanson, R., and Dobrovitski, V. V., “Comparison of dynamical decoupling protocols for a nitrogen-vacancy center in diamond,” *Phys. Rev. B* **85**(15), 155204 (2012).
- [39] Childress, L., Dutt, M. V. G., Taylor, J. M., Zibrov, A. S., Jelezko, F., Wrachtrup, J., Hemmer, P. R., and Lukin, M. D., “Coherent Dynamics of Coupled Electron and Nuclear Spin Qubits in Diamond,” *Science* **314**(5797), 281–285 (2006).
- [40] Stanwix, P. L., Pham, L. M., Maze, J. R., Le Sage, D., Yeung, T. K., Cappellaro, P., Hemmer, P. R., Yacoby, A., Lukin, M. D., and Walsworth, R. L., “Coherence of nitrogen-vacancy electronic spin ensembles in diamond,” *Phys. Rev. B* **82**(20), 201201 (2010).
- [41] Maze, J. R., Taylor, J. M., and Lukin, M. D., “Electron spin decoherence of single nitrogen-vacancy defects in diamond,” *Phys. Rev. B* **78**(9), 094303 (2008).
- [42] Abobeih, M. H., Cramer, J., Bakker, M. A., Kalb, N., Markham, M., Twitchen, D. J., and Taminiau, T. H., “One-second coherence for a single electron spin coupled to a multi-qubit nuclear-spin environment,” *Nat. Commun.* **9**, 2552 (2018).
- [43] Rondin, L., Dantelle, G., Slablab, A., Grosshans, F., Treussart, F., Bergonzo, P., Perruchas, S., Gacoin, T., Chaigneau, M., Chang, H.-C., Jacques, V., and Roch, J.-F., “Surface-induced charge state conversion of nitrogen-vacancy defects in nanodiamonds,” *Phys. Rev. B* **82**(11), 115449 (2010).
- [44] Andrich, P., Alemán, B. J., Lee, J. C., Ohno, K., de las Casas, C. F., Heremans, F. J., Hu, E. L., and Awschalom, D. D., “Engineered Micro- and Nanoscale Diamonds as Mobile Probes for High-Resolution Sensing in Fluid,” *Nano Lett.* **14**(9), 4959–4964 (2014).
- [45] D’Haenens-Johansson, U. F. S., Edmonds, A. M., Newton, M. E., Goss, J. P., Briddon, P. R., Baker, J. M., Martineau, P. M., Khan, R. U. A., Twitchen, D. J., and Williams, S. D., “EPR of a defect in CVD diamond involving both silicon and hydrogen that shows preferential alignment,” *Phys. Rev. B* **82**(15), 155205 (2010).
- [46] Edmonds, A. M., Hart, C. A., Turner, M. J., Colard, P.-O., Schloss, J. M., Olsson, K. S., Trubko, R., Markham, M. L., Rathmill, A., Horne-Smith, B., Lew, W., Manickam, A., Bruce, S., Kaup, P. G., Russo, J. C., DiMario, M. J., South, J. T., Hansen, J. T., Twitchen, D. J., and Walsworth, R. L., “Characterisation of CVD diamond with high concentrations of nitrogen for magnetic-field sensing applications,” *Mater. Quantum. Technol.* **1**(2), 025001 (2021).

- [47] van Dam, S. B., Walsh, M., Degen, M. J., Bersin, E., Mouradian, S. L., Galiullin, A., Ruf, M., IJspeert, M., Taminiau, T. H., Hanson, R., and Englund, D. R., “Optical coherence of diamond nitrogen-vacancy centers formed by ion implantation and annealing,” *Phys. Rev. B* **99**(16), 161203 (2019).
- [48] Chen, Y.-C., Salter, P. S., Knauer, S., Weng, L., Frangeskou, A. C., Stephen, C. J., Ishmael, S. N., Dolan, P. R., Johnson, S., Green, B. L., Morley, G. W., Newton, M. E., Rarity, J. G., Booth, M. J., and Smith, J. M., “Laser writing of coherent colour centres in diamond,” *Nat. Photonics* **11**(2), 77–80 (2017).
- [49] Capelli, M., Heffernan, A. H., Ohshima, T., Abe, H., Jeske, J., Hope, A., Greentree, A. D., Reineck, P., and Gibson, B. C., “Increased nitrogen-vacancy centre creation yield in diamond through electron beam irradiation at high temperature,” *Carbon* **143**, 714–719 (2019).
- [50] Botsoa, J., Sauvage, T., Adam, M.-P., Desgardin, P., Leoni, E., Courtois, B., Treussart, F., and Barthe, M.-F., “Optimal conditions for NV⁻ center formation in type-1b diamond studied using photoluminescence and positron annihilation spectroscopies,” *Phys. Rev. B* **84**(12), 125209 (2011).
- [51] Orwa, J. O., Greentree, A. D., Aharonovich, I., Alves, A. D. C., van Donkelaar, J., Stacey, A., and Prawer, S., “Fabrication of single optical centres in diamond—a review,” *J. Lumin.* **130**(9), 1646–1654 (2010).
- [52] Chu, Y., de Leon, N. P., Shields, B. J., Hausmann, B., Evans, R., Togan, E., Burek, M. J., Markham, M., Stacey, A., Zibrov, A. S., Yacoby, A., Twitchen, D. J., Loncar, M., Park, H., Maletinsky, P., and Lukin, M. D., “Coherent Optical Transitions in Implanted Nitrogen Vacancy Centers,” *Nano Lett.* **14**(4), 1982–1986 (2014).
- [53] Chen, Y.-C., Griffiths, B., Weng, L., Nicley, S. S., Ishmael, S. N., Lekhai, Y., Johnson, S., Stephen, C. J., Green, B. L., Morley, G. W., Newton, M. E., Booth, M. J., Salter, P. S., and Smith, J. M., “Laser writing of individual nitrogen-vacancy defects in diamond with near-unity yield,” *Optica* **6**(5), 662 (2019).
- [54] Knowles, H. S., Kara, D. M., and Atatüre, M., “Observing bulk diamond spin coherence in high-purity nanodiamonds,” *Nat. Mater.* **13**(1), 21–25 (2014).
- [55] Frangeskou, A. C., Rahman, A. T. M. A., Gines, L., Mandal, S., Williams, O. A., Barker, P. F., and Morley, G. W., “Pure nanodiamonds for levitated optomechanics in vacuum,” *New J. Phys.* **20**(4), 043016 (2018).
- [56] Ginés, L., Mandal, S., Morgan, D. J., Lewis, R., Davies, P. R., Borri, P., Morley, G. W., and Williams, O. A., “Production of metal-free diamond nanoparticles,” *ACS Omega* **3**(11), 16099–16104 (2018).
- [57] Hsu, J.-F., Ji, P., Lewandowski, C. W., and D’Urso, B., “Cooling the Motion of Diamond Nanocrystals in a Magneto-Gravitational Trap in High Vacuum,” *Sci. Rep.* **6**, 30125 (2016).
- [58] Haslinger, P., Dörre, N., Geyer, P., Rodewald, J., Nimmrichter, S., and Arndt, M., “A universal matter-wave interferometer with optical ionization gratings in the time domain,” *Nature Phys.* **9**(3), 144–148 (2013).
- [59] Eibenberger, S., Gerlich, S., Arndt, M., Mayor, M., and Tüxen, J., “Matter-wave interference of particles selected from a molecular library with masses exceeding 10 000 amu,” *Phys. Chem. Chem. Phys.* **15**(35), 14696 (2013).
- [60] Fein, Y. Y., Geyer, P., Zwick, P., Kiałka, F., Pedalino, S., Mayor, M., Gerlich, S., and Arndt, M., “Quantum superposition of molecules beyond 25 kDa,” *Nat. Phys.* **15**(12), 1242–1245 (2019).
- [61] Bassi, A., Lochan, K., Satin, S., Singh, T. P., and Ulbricht, H., “Models of wave-function collapse, underlying theories, and experimental tests,” *Rev. Mod. Phys.* **85**(2), 471–527 (2013).
- [62] Fröwis, F., Sekatski, P., Dür, W., Gisin, N., and Sangouard, N., “Macroscopic quantum states: Measures, fragility, and implementations,” *Rev. Mod. Phys.* **90**(2), 025004 (2018).
- [63] Nimmrichter, S. and Hornberger, K., “Macroscopicity of Mechanical Quantum Superposition States,” *Phys. Rev. Lett.* **110**(16), 160403 (2013).
- [64] Marshman, R. J., Mazumdar, A., and Bose, S., “Locality and entanglement in table-top testing of the quantum nature of linearized gravity,” *Phys. Rev. A* **101**(5), 052110 (2020).
- [65] Keil, M., Machluf, S., Margalit, Y., Zhou, Z., Amit, O., Dobkowski, O., Japha, Y., Moukouri, S., Rohrlich, D., Binstock, Z., Bar-Haim, Y., Givon, M., Groswasser, D., Meir, Y., and Folman, R., “Stern-gerlach interferometry with the atom chip,” in [*Molecular Beams in Physics and Chemistry: From Otto Stern’s Pioneering Exploits to Present-Day Feats*], Friedrich, B. and Schmidt-Böcking, H., eds., 263–301, Springer International Publishing, Cham (2021).

- [66] Margalit, Y., Dobkowski, O., Zhou, Z., Amit, O., Japha, Y., Moukouri, S., Rohrich, D., Mazumdar, A., Bose, S., Henkel, C., and Folman, R., “Realization of a complete Stern-Gerlach interferometer: Toward a test of quantum gravity,” *Sci. Adv.* **7**(22), eabg2879 (2021).
- [67] Marshman, R. J., Mazumdar, A., Folman, R., and Bose, S., “Large Splitting Massive Schrödinger Kittens,” arXiv:2105.01094 (2021).
- [68] Chevalier, H., Paige, A. J., and Kim, M. S., “Witnessing the nonclassical nature of gravity in the presence of unknown interactions,” *Phys. Rev. A* **102**(2), 022428 (2020).
- [69] Toroš, M., Mazumdar, A., and Bose, S., “Loss of coherence of matter-wave interferometer from fluctuating graviton bath,” arXiv:2008.08609 (2020).
- [70] Toroš, M., van de Kamp, T. W., Marshman, R. J., Kim, M. S., Mazumdar, A., and Bose, S., “Relative acceleration noise mitigation for nanocrystal matter-wave interferometry: Applications to entangling masses via quantum gravity,” *Phys. Rev. Res.* **3**(2), 023178 (2021).
- [71] van de Kamp, T. W., Marshman, R. J., Bose, S., and Mazumdar, A., “Quantum gravity witness via entanglement of masses: Casimir screening,” *Phys. Rev. A* **102**(6), 062807 (2020).
- [72] Neukirch, L. P., Gieseler, J., Quidant, R., Novotny, L., and Nick Vamivakas, A., “Observation of nitrogen vacancy photoluminescence from an optically levitated nanodiamond,” *Opt. Lett.* **38**(16), 2976 (2013).
- [73] Neukirch, L. P., von Haartman, E., Rosenholm, J. M., and Nick Vamivakas, A., “Multi-dimensional single-spin nano-optomechanics with a levitated nanodiamond,” *Nat. Photonics* **9**(10), 653–657 (2015).
- [74] Hoang, T. M., Ahn, J., Bang, J., and Li, T., “Electron spin control of optically levitated nanodiamonds in vacuum,” *Nat. Commun.* **7**, 12250 (2016).
- [75] Pettit, R. M., Neukirch, L. P., Zhang, Y., and Nick Vamivakas, A., “Coherent control of a single nitrogen-vacancy center spin in optically levitated nanodiamond,” *J. Opt. Soc. Am. B* **34**(6), C31 (2017).
- [76] Delord, T., Nicolas, L., Schwab, L., and Hétet, G., “Electron spin resonance from NV centers in diamonds levitating in an ion trap,” *New J. Phys.* **19**(3), 033031 (2017).
- [77] Conangla, G. P., Schell, A. W., Rica, R. A., and Quidant, R., “Motion Control and Optical Interrogation of a Levitating Single Nitrogen Vacancy in Vacuum,” *Nano Lett.* **18**(6), 3956–3961 (2018).
- [78] Kuhlicke, A., Schell, A. W., Zoll, J., and Benson, O., “Nitrogen vacancy center fluorescence from a submicron diamond cluster levitated in a linear quadrupole ion trap,” *Appl. Phys. Lett.* **105**(7), 073101 (2014).
- [79] Delord, T., Nicolas, L., Bodini, M., and Hétet, G., “Diamonds levitating in a Paul trap under vacuum: Measurements of laser-induced heating via NV center thermometry,” *Appl. Phys. Lett.* **111**(1), 013101 (2017).
- [80] Delord, T., Huillery, P., Schwab, L., Nicolas, L., Lecordier, L., and Hétet, G., “Ramsey Interferences and Spin Echoes from Electron Spins Inside a Levitating Macroscopic Particle,” *Phys. Rev. Lett.* **121**(5), 053602 (2018).
- [81] Delord, T., Huillery, P., Nicolas, L., and Hétet, G., “Spin-cooling of the motion of a trapped diamond,” *Nature* **580**, 56–59 (2020).
- [82] Berry, M. V. and Geim, A. K., “Of flying frogs and levitrons,” *Eur. J. Phys.* **18**(4), 307–313 (1997).
- [83] O’Brien, M. C., Dunn, S., Downes, J. E., and Twamley, J., “Magneto-mechanical trapping of micro-diamonds at low pressures,” *Appl. Phys. Lett.* **114**(5), 053103 (2019).